DPNU 00-24
August 2000

# Schematic Method for Estimation of CP Asymmetry in Neutrino Oscillation

K. Kimura[a] and A. Takamura[bc]

[a,b]*Department of Physics, Nagoya University*
*Nagoya 464-8602, Japan*

[c]*Department of Mathematics, Toyota National Collage of Technology Eisei-cho 2-1, Toyota-shi, 471-8525, Japan*

## Abstract

Within the framework of three generations of leptons the schematical method for estimating CP asymmetry in neutrino oscillations is considered. We introduce a unitarity triangle corresponding to $\nu_e$-$\nu_\mu$ oscillation, in addition, we show that it is convenient for the estimation to define another new triangle. CP asymmetry is determined by the difference between the shapes of a unitarity triangle and new triangle. As results, (i) we show that CP asymmetry becomes maximal if the shapes of these two triangles are the same. (ii) We can easily estimate $L/E$ which leads almost 100% asymmetry using this. (iii) In $\nu_e$-$\nu_\mu$ oscillation with $\sin^2 2\theta_{13} \simeq 0.04$, we obtain about 90% asymmetry for LMA MSW scenario and 3% asymmetry for SMA MSW scenario within long baseline neutrino expriments to be realized in near future.

[a]Email: kimukei@eken.phys.nagoya-u.ac.jp
[b]Email: takamura@eken.phys.nagoya-u.ac.jp

# 1 Introduction

Recent atmospheric neutrino experiments [1] strongly suggest $\nu_\mu$-$\nu_\tau$ oscillations with large mixing. On the other hand, solar neutrino experiments [2] also suggest $\nu_e$-$\nu_\mu$ or $\nu_e$-$\nu_\tau$ oscillations. These results imply the participation of at least three generations in the lepton sector.

In the framework of three generations, it is natural to consider CP violation in neutrino oscillations. The estimation of CP phase in the lepton sector, if it exists, is very important to construct the physics beyond the Standard Model. As 1-3 mixing and 1-2 mass difference are small, it is difficult to observe CP violation effects at present experiments. However, there are following favorable points to observe CP violation in neutrino oscillations. First, various long baseline experiments with high intensity neutrino beams are planned in near future. There are mainly two kinds of experiments with high energy neutrino like neutrino factory experiments [3], and with low energy neutrino like PRISM [4]. Second, the appearence of large 2-3 mixing discovered by Super-Kamiokande Collaboration provides the possibilities of large CP violation in the lepton sector. This is contrast to CP violation in the quark sector with small 2-3 mixing. Considering of this point, CP violation in neutrino oscillations have been investigated by many authors [5, 6].

In this work, we propose the schematical approach to estimate CP asymmetry in neutrino oscillation defined by

$$A_{CP} \;=\; \frac{\Delta P_{\not{CP}}}{\Delta P_{CP}} = \frac{P(\nu_\alpha \to \nu_\beta) - P(\bar{\nu}_\alpha \to \bar{\nu}_\beta)}{P(\nu_\alpha \to \nu_\beta) + P(\bar{\nu}_\alpha \to \bar{\nu}_\beta)}, \tag{1}$$

where $\Delta P_{CP}$ is CP-conserving part and $\Delta P_{\not{CP}}$ is CP-violating part. We introduce a unitarity triangle in the lepton sector and another new triangle to estimate $A_{CP}$. We explore the condition in which $A_{CP}$ takes the value as large as possible using the geometry of the two triangles. From the condition, $L/E$ which leads the almost 100% asymmetry can be estimated easily, where $L$ is the baseline length and $E$ is the neutrino energy. In the case of LMA and SMA MSW scenarios, we derive such $L/E$ and estimate whether large $A_{CP}$ is realized in near future experiments.

# 2 Neutrino Oscillations in Three Generation

In this section we consider the neutrino oscillation in three generation and represent transition probability from one flavor to another flavor using the components of the Maki-Nakagawa-Sakata matrix (MNS matrix) [7].

In vacuum, flavor eigenstates $\nu_\alpha\,(\alpha = e, \mu, \tau)$ are related to mass eigenstates $\nu_i (i = 1, 2, 3)$, which have the mass eigenvalues $m_i$, by unitary transformation,

$$\nu_\alpha = U_{\alpha i}\nu_i, \tag{2}$$

where $U_{\alpha i}$ is the MNS matrix.

Transition probability from $\nu_\alpha$ to $\nu_\beta (\alpha \neq \beta)$ after having traveled a distance $L$ is given by

$$P(\nu_\alpha \to \nu_\beta) = -4 \sum_{i<j}^{3} \mathrm{Re}(J^{ij}_{\alpha\beta}) \sin^2 \phi_{ij} - 2JK, \tag{3}$$

where

$$J^{ij}_{\alpha\beta} \equiv U_{\alpha i} U^*_{\beta i} U^*_{\alpha j} U_{\beta j}, \quad \phi_{ij} \equiv \kappa \Delta m^2_{ij} L/E = \kappa (m^2_i - m^2_j) L/E, \tag{4}$$

with $\kappa = 1/4$ in natural units or $\kappa = 1.27$ in GeV per km and eV$^2$ and

$$K \equiv 4 \sin \phi_{12} \sin \phi_{23} \sin \phi_{31}, \quad J \equiv \mathrm{Im}(J^{12}_{e\mu}). \tag{5}$$

$J$ is so called, Jarlscog factor [8], $\mathrm{Im}(J^{ij}_{\alpha\beta})$ obtained by the (anti-) cyclic permutation of ($e$, $\mu$) and (1,2) are all equal to $(-)J$.

# 3 CP Asymmetry and Two Kinds of Triangles

In this section, we would like to investigate CP asymmetry obtained from (3) schematically. We introduce two kinds of triangles. One is a unitarity triangle defined by $J^{ij}_{\alpha\beta}$ in (3), which we call MNS triangle. The other is another new triangle defined by $\phi_{ij}$ also in (3), which we call oscillation triangle. We describe the definitions of the two kinds of triangles after we present our main results. CP asymmetry is presented by using the sides of the two kinds of triangles as

$$A_{CP} = \frac{P(\nu_\alpha \to \nu_\beta) - P(\bar{\nu}_\alpha \to \bar{\nu}_\beta)}{P(\nu_\alpha \to \nu_\beta) + P(\bar{\nu}_\alpha \to \bar{\nu}_\beta)} = \pm \frac{1}{\sqrt{1+D}} \tag{6}$$

where $D$ is defined by

$$\begin{aligned} 4J^2K^2D \equiv\ & (|b|^2|n|^2 - |c|^2|m|^2)(|a|^2|n|^2 - |c|^2|l|^2) \\ + & (|c|^2|l|^2 - |a|^2|n|^2)(|b|^2|l|^2 - |a|^2|m|^2) \\ + & (|a|^2|m|^2 - |b|^2|l|^2)(|c|^2|m|^2 - |b|^2|n|^2), \end{aligned} \tag{7}$$

and $|a|$, $|b|$ and $|c|$ are the sides of an MNS triangle and $|l|$, $|m|$ and $|n|$ are an oscillation triangle as in Fig.1.

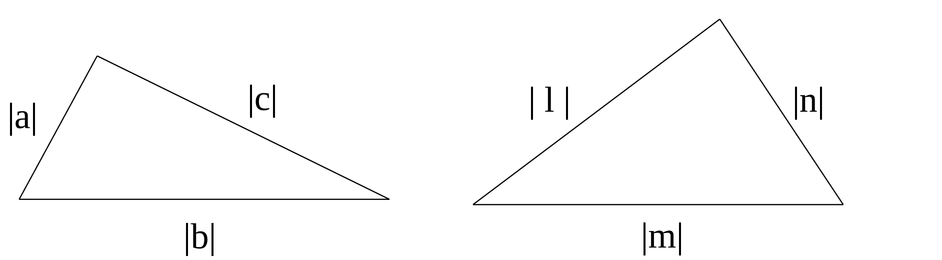


Fig. 1(a) an MNS triangle Fig. 1(b) an oscillation triangle

The definition of the two kinds of triangles are as follows. At first, we define MNS triangle by introducing complex numbers, $a$, $b$ and $c$ as

$$a \equiv U^*_{\alpha 1} U_{\beta 1}, \qquad b \equiv U^*_{\alpha 2} U_{\beta 2}, \qquad c \equiv U^*_{\alpha 3} U_{\beta 3}, \tag{8}$$

whose absolute values mean the length of the three sides of an MNS triangle because of unitarity condition,

$$U^*_{\alpha 1} U_{\beta 1} + U^*_{\alpha 2} U_{\beta 2} + U^*_{\alpha 3} U_{\beta 3} = 0. \tag{9}$$

$J^{ij}_{\alpha\beta}$ of (3) are rewritten with the three sides of an MNS triangle from the relations such as

$$J^{12}_{\alpha\beta} = a^* b, \quad J^{23}_{\alpha\beta} = b^* c, \quad J^{31}_{\alpha\beta} = c^* a. \tag{10}$$

Next, we define oscillation triangle. We choose one side (the base of the triangle whose length has no physical meaning and is chosen arbitrary) and two base angles, $\phi_{21}$ and $\phi_{32}$, as shown in Fig.2 to define the oscillation triangle. Note that while the base is constant in baseline length, $L$, both $\phi_{21}$ and $\phi_{32}$ are dependent on $L$ from the definition. It should be emphasized that the position of point A depends on $L$ and point A is located above or below the base line of the triangle. Oscillation triangles belong to either two classes like in Fig.2. In Case I point A is located above the base like in Fig.2(a) and in Case II point A is located below the base like in Fig.2(b).

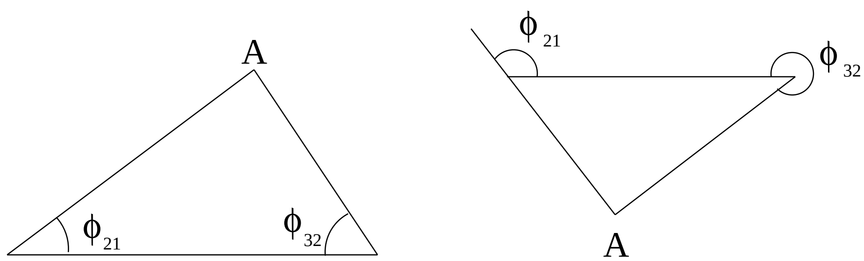


Fig. 2(a) Case I

Fig. 2(b) Case II

The interior angles of the oscillation triangles, $\eta_1$, $\eta_2$ and $\eta_3$, are determined as follows in each cases.

**Case I** In Fig.2(a) the interior angles are

$$\begin{cases} \eta_1 = \phi_{32} - N\pi \\ \eta_2 = -\phi_{31} + (N + N' + 1)\pi \\ \eta_3 = \phi_{21} - N'\pi \end{cases}, \tag{11}$$

where $N$ and $N'$ are integers which can be chosen to make $\eta_1$ and $\eta_3$ between 0 and $\pi$.

**Case II** In Fig.2(b) the interior angles are

$$\begin{cases} \eta_1 = -\phi_{32} + N\pi \\ \eta_2 = \phi_{31} + (1 - N - N')\pi \\ \eta_3 = -\phi_{21} + N'\pi \end{cases} , \tag{12}$$

where $N$ and $N'$ are also integers which can be chosen to make $\eta_1$ and $\eta_3$ between 0 and $\pi$.

As the transition probability of (3) depends only on angles of the oscilletion triangle, the shape is important, on the other hand, the scale and the position in complex plane have nothing to do with the magnitude of transition probability. We choose the radius of the circumcircle as 1 and fix the oscillation triangles in complex plane as in Fig. 3 making use of the arbitrariness of the scale and the position. The three sides, $l$, $m$ and $n$, are defined using complex numbers like

$$l = 2\sin\eta_1(\cos\eta_3 \mp i\sin\eta_3), \quad m = 2\sin\eta_2, \quad n = 2\sin\eta_3(-\cos\eta_1 \pm i\sin\eta_1) \tag{13}$$

as the opposite side of the three angles, where the sign correspond to case I and case II.

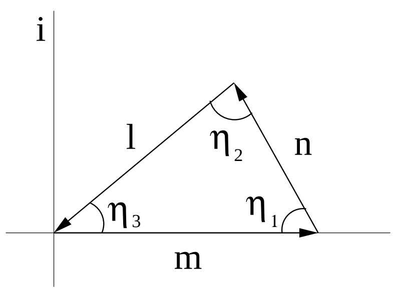


Fig. 3(a) Case I

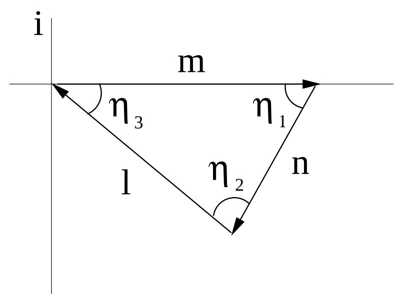


Fig. 3(b) Case II

We replace $\phi_{ij}$ of (3) with the sides as

$$\sin^2\phi_{23} = |l|^2/4, \quad \sin^2\phi_{31} = |m|^2/4, \quad \sin^2\phi_{12} = |n|^2/4. \tag{14}$$

Furthermore, the introduction of complex numbers as the three sides makes possible to represent $K$ as the same form in both cases like

$$K = \pm 4\sin\eta_1\sin\eta_2\sin\eta_3 = \mathrm{Im}(l^*m) = \mathrm{Im}(m^*n) = \mathrm{Im}(n^*l), \tag{15}$$

where plus and minus sign correspond to the Case I and Case II respectively and the absolute value of $K$ means the twice of the area of the oscillation triangle.

After the definition of the two kinds of triangles described above, we rewrite CP asymmetry,

$$A_{CP} = \frac{\Delta P_{\cancel{CP}}}{\Delta P_{CP}} = \frac{P(\nu_\alpha \to \nu_\beta) - P(\bar{\nu}_\alpha \to \bar{\nu}_\beta)}{P(\nu_\alpha \to \nu_\beta) + P(\bar{\nu}_\alpha \to \bar{\nu}_\beta)}, \tag{16}$$

using the sides of two kinds of triangles. As $P(\bar{\nu}_\alpha \to \bar{\nu}_\beta)$ are obtained by the replacement $U \to U^*$ in $P(\nu_\alpha \to \nu_\beta)$, CP-violating part and CP-conserving part are

$$\begin{aligned} \Delta P_{\not{CP}} &= -4JK, & (17) \\ \Delta P_{CP} &= -2\{\mathrm{Re}(a^*b)|n|^2 + \mathrm{Re}(b^*c)|l|^2 + \mathrm{Re}(c^*a)|m|^2\}, & (18) \end{aligned}$$

where (10) and (14) are used. Furthermore, CP-conserving part is rewritten as

$$\begin{aligned} (\Delta P_{CP}/2)^2 &= 4J^2K^2 + (|b|^2|n|^2 - |c|^2|m|^2)(|a|^2|n|^2 - |c|^2|l|^2) \\ &\quad + (|c|^2|l|^2 - |a|^2|n|^2)(|b|^2|l|^2 - |a|^2|m|^2) \\ &\quad + (|a|^2|m|^2 - |b|^2|l|^2)(|c|^2|m|^2 - |b|^2|n|^2) \qquad (19) \end{aligned}$$

using the theorems about the sides and angles of triangles. The important relations of (6) and (7) are obtained from (17) and (19), where $J \neq 0$ and $K \neq 0$ are used. At the end of this section, we show the condition which gives the maximal CP asymmetry. For the purpose, we consider another representation of $D$ like

$$\begin{aligned} 4J^2K^2D &= \frac{1}{|l|^2|m|^2}\left(|c|^2|l|^2|m|^2 - \mathrm{Re}(m^*n)|b|^2|l|^2 - \mathrm{Re}(n^*l)|a|^2|m|^2\right)^2 \\ &\quad + \frac{K^2}{4|l|^2|m|^2}(|a|^2|m|^2 - |b|^2|l|^2)^2 \geq 0, \qquad (20) \end{aligned}$$

and from the equality condition of (20) we have 100% asymmetry,

$$A_{CP} = \pm 1, \qquad (21)$$

in the case that the ratio of the sides of an MNS triangle and an oscillation triangle is

$$|a| : |b| : |c| = |l| : |m| : |n|, \qquad (22)$$

namely the shapes of the two triangles are the same. Conversly, CP asymmetry is not 100% if the two triangles are not the same shape, then the differences of the shapes determine the magnitude of CP asymmetry.

# 4 Estimation of CP Asymmetry

In this section, let us apply the schematic method obtained in the previous section for $\nu_e$-$\nu_\mu$ oscillation and estimate the magnitude of CP asymmetry. In the following discussions, the representative set of parameters as in Table.1 [9] are used in LMA MSW and SMA MSW scenarios as examples. Only upper bound, $\sin^2 2\theta_{13} < 0.2$, is given by CHOOZ experiment [10] about 1-3 mixing. Later we consider how $A_{CP}$ changes when $\sin\theta_{13}$ changes.

| Scenario | $\Delta m_{32}^2(\mathrm{eV}^2)$ | $\Delta m_{21}^2(\mathrm{eV}^2)$ | $\sin^2 2\theta_{23}$ | $\sin^2 2\theta_{12}$ | $\sin^2 2\theta_{13}$ | $\delta$ |
|---|---|---|---|---|---|---|
| | (atmos) | (solar) | (atmos) | (solar) | | |
| LMA MSW | $3.5 \times 10^{-3}$ | $5 \times 10^{-5}$ | 1 | 0.8 | 0.04 | $\pi/2$ |
| SMA MSW | $3.5 \times 10^{-3}$ | $1 \times 10^{-5}$ | 1 | 0.01 | 0.04 | $\pi/2$ |

Table 1: reference set of mass square differences, mixing angles and CP phase

There are two distinct mass differences in three generations and they are set to explain the atmospheric and the solar neutrino deficit. The form of the MNS matrices in these two scenarios are

$$U(\mathrm{LMA}) = \begin{pmatrix} 0.846 & 0.523 & -0.101i \\ -0.372 - 0.060i & 0.602 - 0.037i & 0.704 \\ 0.372 - 0.060i & -0.602 - 0.037i & 0.704 \end{pmatrix} \tag{23}$$

for LMA MSW scenario and

$$U(\mathrm{SMA}) = \begin{pmatrix} 0.994 & 0.050 & -0.101i \\ -0.035 - 0.071i & 0.706 - 0.004i & 0.704 \\ 0.035 - 0.071i & -0.706 - 0.004i & 0.704 \end{pmatrix} \tag{24}$$

for SMA MSW scenario. In each cases, the MNS triangle corresponding to $\nu_e$-$\nu_\mu$ oscillation is shown in Fig. 4(a) and Fig. 4(b). The three sides of the MNS triangle are

$$(|a|, |b|, |c|) = \begin{cases} (0.32, 0.32, 0.071) & \text{for LMA MSW} \\ (0.079, 0.035, 0.071) & \text{for SMA MSW} \end{cases} \tag{25}$$

and three angles are

$$(\psi_1, \psi_2, \psi_3) = \begin{cases} (1.46, 1.46, 0.22) & \text{for LMA MSW} \\ (1.56, 0.46, 1.12) & \text{for SMA MSW} \end{cases} . \tag{26}$$

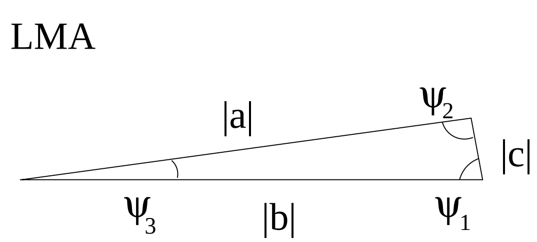


Fig. 4(a) MNS triangle for LMA MSW scenario

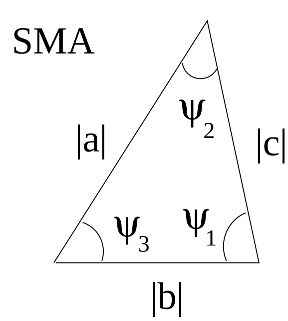


Fig. 4(b) MNS triangle for SMA MSW scenario

At first, let us show that the smallest $L/E$ which gives the almost 100% asymmetry is estimated as

$$\frac{L(\mathrm{km})}{E(\mathrm{GeV})} = \left\{ \begin{array}{ll} 3200 & \text{for LMA MSW} \\ 88000 & \text{for SMA MSW} \end{array} \right. , \tag{27}$$

with the schematic method. These values are derived as following two steps. At first, choose $L/E$ such that $\eta_3 = \phi_{21} = \psi_3$, that is

$$\phi_{21} = \frac{1.27\Delta m_{21}^2 L}{E} = \left\{ \begin{array}{ll} 0.22 & \text{for LMA MSW} \\ 1.12 & \text{for SMA MSW} \end{array} \right. . \tag{28}$$

Second, change the value of $L/E$ obtained from (28) a little so that $\eta_1 = \phi_{32} - N\pi = \psi_1$, that is

$$\phi_{32} = \frac{1.27\Delta m_{32}^2 L}{E} = \left\{ \begin{array}{ll} 1.46 + N_L\pi & \text{for LMA MSW} \\ 1.56 + N_S\pi & \text{for SMA MSW} \end{array} \right. , \tag{29}$$

where $N_L = 4$ and $N_S = 124$ for the $L/E$ determined by (28). There is little change for the angle $\eta_3$ set at first by the second operation because $\phi_{32}$ and $\phi_{31}$ change rapidly compared to $\phi_{21}$. Thus, we can easily estimate $L/E$ which gives almost 100% asymmetry as (27) by choosing the oscillation triangle to be the almost same shape as the MNS triangle in Fig. 4.

Next, let us roughly estimate whether $L/E$ of (27) can be realized in future experiments taking the two kinds of experiments as examples. First, in the experiments of neutrino factory [3], suppose that the energy of neutrino beam is 5 GeV and the baseline length is about 7400 km from Fermilab to Gran Sasso. Second, in the experiments of PRISM [4], suppose that the energy of the neutrino beam is 100 MeV and the baseline length is $L \sim 250$ km from KEK to Super-Kamiokande. The value of $L(\mathrm{km})/E(\mathrm{GeV})$ realized in the two kinds of future experiments are

$$\frac{L(\mathrm{km})}{E(\mathrm{GeV})} \sim \left\{ \begin{array}{ll} 1500 & \text{for neutrino factory} \\ 2500 & \text{for PRISM} \end{array} \right. . \tag{30}$$

These values of $L(\mathrm{km})/E(\mathrm{GeV})$ are close to the value of (27) for LMA MSW scenario. Therefore, it is expected to obtain rather large CP asymmetry. Actually at the value of $L(\mathrm{km})/E(\mathrm{GeV}) \sim 2500$ we obtain

$$A_{CP} \sim \left\{ \begin{array}{ll} 90\% & \text{for LMA MSW} \\ 3\% & \text{for SMA MSW} \end{array} \right. , \tag{31}$$

where

$$(|l|, |m|, |n|) = \left\{ \begin{array}{ll} (1.99, 1.92, 0.32) & \text{for LMA MSW} \\ (1.99, 1.98, 0.063) & \text{for SMA MSW.} \end{array} \right. , \tag{32}$$

derived from the definition of $\phi_{ij}$ and (14) are used.

Finally, let us consider how the magnitude of $A_{CP}$ is changed by $\sin\theta_{13}$. If $\sin\theta_{13}$ is smaller than the value we choose, $|c|$ and the angle $\gamma$ corresponding to $|c|$ of the MNS triangle is also small. Eq.(28) leads to small $L/E$ which gives almost 100% asymmetry according to the smallness of $\gamma$. Therefore, rather large $A_{CP}$ may be realized not only in LMA MSW scenario but also in SMA MSW scenario if $\sin\theta_{13}$ is small. However, as small $\gamma$ means the squashed MNS triangle, $J$ and therefore $\Delta P_{\not{CP}}$ become also small. We need the beam which has high intensity enough to compensate the smallness of $\Delta P_{\not{CP}}$ to observe $A_{CP}$.

# 5 Summary and Discussions

In the framework of three generations we have mainly investigated CP asymmetry in neutrino oscillations. The main results of this paper are following;

(i) We propose the scematical method to estimate the magnitude of $A_{CP}$. $A_{CP}$ is calculated from the length of three sides of an MNS triangle and an oscillation triangle. $A_{CP}$ takes the maximal value in the case that the shapes of the two triangles are the same.

(ii) In vacuum $\nu_e$-$\nu_\mu$ oscillation, we obtain almost 100% asymmetry in $L(\text{km})/E(\text{GeV}) \sim 3200$ for LMA MSW scenario and in $L(\text{km})/E(\text{GeV}) \sim 88000$ for SMA MSW scenario.

(iii) In PRISM experiment to be expected to realize near future, we obtain about $A_{CP} \sim 90\%$ for LMA MSW scenario and $A_{CP} \sim 3\%$ for SMA MSW scenario with $\sin^2 2\theta_{13} \simeq 0.04$.

Finally we note the prospect in future. In order to determine the magnitude of CP asymmetry we need to estimate other parameters of the MNS matrix as precise as possible. Furthermore, the mass differences and mixing angles are changed by the earth matter effect in practical long baseline neutrino experiments. We would like to investigate how large the earth matter effect is in CP violation and in what region our results are ineffective in the paper to be prepared. We will also study $A_{CP}$ averaging in the neutrino energy and the baseline length in order to estimate CP violating effects in practical experiments. If the limitation of the energy resolution is improved, the CP violating signals become more sharp. We should consider the better method to obtain the CP violating signal as sharp as possible. In addition, we investigate other MNS triangles in the next paper.

# Acknowledgement

The authors would like to thank Prof. A. I. Sanda for useful discussions and fruitful comments. We would like to thank Prof. Y. Sugiyama for careful reading of manuscript.

## References


[1] Super-Kamiokande Collabolation, Y. Fukuda et al., Phys. Rev. Lett. 81, (1998) 1562, Phys. Lett. B433, (1998) 9, Phys. Lett. B436, (1998) 33, Phys. Rev. Lett. 82, (1999) 2644; IMB collaboration, R. Becker-Szendy et al., Nucl. Phys. Proc. Suppl. 38B, (1995) 331; Soudan-2 collaboration, W. W. M. Allison et al., Phys. Lett. B391, (1997) 491; MACRO collaboration, M. Ambrosio et al., Phys. Lett. B434, (1998) 451.

[2] GALLEX Collaboration, W. Hampel et al., Phys. Lett. B447, (1999) 127; SAGE Collaboration, J. N. Abdurashitov et al., astro-ph/9907113; Homestake Collaboration, B. T. Cleveland et al., Astrophys. J. 496, (1998) 505; Super-Kamiokande Collaboration, Y. Fukuda et al., Phys. Rev. Lett. 82, (1999) 1810, ibid. 82, (1999) 2430.

[3] S. H. Geer, Phys. Rev. D57, (1998) 6989.

[4] Y. Kuno and Y. Mori, Talked at the ICFA/FCFA Workshop "Neutrino Factories based on Muon Strage Ring", July 1999; Y. Kuno, in Proceedings of the Workshop on High Intensity Secondary Beam with Phase Rotation.

[5] M. Koike and J. Sato, hep-ph/9909469v2; J. Sato, hep-ph/9910442; H. Minakata and H. Nunokawa, hep-ph/0004114; O. Yasuda, Acta Phys. Polon. B30 (1999) 3089; P. F. Harrison and W. G. Scott, hep-ph/9912435; V. Barger, S. Geer, R. Raja and K. Whisnant, hep-ph/0003184.

[6] M. Tanimoto, Phys. Lett. B462 (1999) 115; A. Kalliomki, J. Maalampi and M. Tanimoto, hep-ph/9909301; A. De Rujula, M. B. Gavela and P. Hernandez, Nucl. Phys. B547 (1999) 21; A. Donini, M. B. Gavela, P. Hernandez and S. Rigolin, hep-ph/9909254; A. Cervera, A. Donini, M. B. Gavela, J. J. Gomez Cadenas, P. Hernandez, O. Mena and S. Rigolin, hep-ph/0002108; K. Dick, M. Freund, M. Lindner and A. Romanino, Nucl. Phys. B562 (1999) 29; A. Romanino, hep-ph/9909425; Z. Xing, hep-ph/0002246.

[7] Z. Maki, M. Nakagawa, S. Sakata, Prog. Theor. Phys. 28 (1962) 870.

[8] C. Jarlscog, Phys. Rev. Lett. 55 (1985) 1839.

[9] See the Fermilab Long-Baseline Workshop web site at http://www.fnal.gov/ projects/ muon-collider/ nu/study/study.html

[10] CHOOZ Collaboration, M. Apollonio et al., Phys. Lett. B420 (1998) 397; ibid., B466 (1999) 415.